

Regulatory T Cells in an Endogenous Mouse Lymphoma Recognize Specific Antigen Peptides and Contribute to Immune Escape



Fatima Ahmetlić^{1,2}, Tanja Riedel², Nadine Hömberg^{1,2}, Vera Bauer¹, Nico Trautwein³, Albert Geishauer^{1,2}, Tim Sparwasser⁴, Stefan Stevanović³, Martin Röcken⁵, and Ralph Mocikat^{1,2}

Abstract

Foxp3⁺ regulatory T cells (Tregs) sustain immune homeostasis and may contribute to immune escape in malignant disease. As a prerequisite for developing immunologic approaches in cancer therapy, it is necessary to understand the ontogeny and the antigenic specificities of tumor-infiltrating Tregs. We addressed this question by using a λ -MYC transgenic mouse model of endogenously arising B-cell lymphoma, which mirrors key features of human Burkitt lymphoma. We show that Foxp3⁺ Tregs suppress antitumor responses in endogenous lymphoma. Ablation of Foxp3⁺ Tregs signif-

icantly delayed tumor development. The ratio of Treg to effector T cells was elevated in growing tumors, which could be ascribed to differential proliferation. The Tregs detected were mainly natural Tregs that apparently recognized self-antigens. We identified MHC class II-restricted nonmutated self-epitopes, which were more prevalent in lymphoma than in normal B cells and could be recognized by Tregs. These epitopes were derived from proteins that are associated with cellular processes related to malignancy and may be overexpressed in the tumor.

Introduction

The immune system is capable of distinguishing harmful pathogens from self-tissues or innocuous environmental factors. CD4⁺ regulatory T cells (Tregs), which are characterized by the expression of surface CD25 and the transcription factor forkhead box p3 (Foxp3), are thought to contribute to immune tolerance, thereby limiting proinflammatory responses in infectious disease and preventing autoaggressive disorders (1–3). Deficiency of Foxp3⁺ Tregs results in T-cell-mediated tissue damage, inflammatory bowel disease, and allergies (4, 5). The suppressive functions exerted by Tregs are mediated by cytokines such as interleukin-10 (IL10) or transforming growth factor- β (TGF β) or by cellular contacts.

The Treg lineage can be subdivided into two subsets: natural Treg cells (nTregs), also known as thymic Treg cells (tTregs), differentiate from potentially self-reactive T-effector cells (Teffs)

upon high-affinity recognition of major histocompatibility complex (MHC) class II-peptide complexes in the thymus, whereas induced Tregs (iTregs) derive from Teffs in the periphery (therefore also known as pTregs) when exposed to antigen (Ag) under tolerogenic conditions (4, 6–8). It was suggested (9) that nTregs can be defined by their expression of Helios, a member of the Ikaros transcription factor family, although this was reported not to be sufficient in subsequent studies (10–12). In the mouse, nTregs express the surface molecule neuropilin-1 (Nrp-1; refs. 13, 14).

Tregs also seem to induce immune tolerance against tumors. The presence of Foxp3⁺ Tregs is associated with suppression of antitumor responses in patients with, e.g., ovarian or colorectal cancer (15, 16). In breast cancer, high Foxp3 expression correlated with poor prognosis (17). The tumor-promoting function of Tregs was demonstrated in mouse models where selective Treg depletion gave rise to enhanced responses against mammary carcinoma or melanoma (18, 19).

Previous studies suggested that the generation of the Treg repertoire is dependent on Ag recognition by T-cell receptors (TCR) and that Tregs differentiated in the thymus receive activating antigenic signals in the periphery (20–23). Little is known, however, of the origin and the Ag specificity of Tregs that are coopted by growing tumors. This knowledge is indispensable for better understanding Treg-associated pathways of tumor immune escape and eventually developing strategies to break immune tolerance.

Because malignant B-cell neoplasia has still a poor prognosis in the clinic, therapeutic regimens that include approaches to overcome immune escape are needed. Therefore, we set out to understand the identity of potentially immunosuppressive Tregs in lymphoma and how they affect tumor growth. As endogenous tumor models more closely reflect the clinical situation and show

¹Helmholtz-Zentrum München, Eigenständige Forschungseinheit Translationale Molekulare Immunologie, München, Germany. ²Helmholtz-Zentrum München, Institut für Molekulare Immunologie, München, Germany. ³Eberhard-Karls-Universität, Interfakultäres Institut für Zellbiologie, Tübingen, Germany. ⁴Institut für Infektionsimmunologie, Twincore, Zentrum für Experimentelle und Klinische Infektionsforschung, Hannover, and Institut für Medizinische Mikrobiologie und Hygiene, Johannes-Gutenberg-Universität, Mainz, Germany. ⁵Eberhard-Karls-Universität, Universitäts-Hautklinik, Tübingen, Germany.

Note: Supplementary data for this article are available at Cancer Immunology Research Online (<http://cancerimmunolres.aacrjournals.org/>).

Corresponding Author: Ralph Mocikat, Helmholtz-Zentrum München, Marchioninistr. 25, D-81377 München, Germany. Phone: 49-89-3187-1302; Fax: 49-89-3187-1300; E-mail: Mocikat@helmholtz-muenchen.de

doi: 10.1158/2326-6066.CIR-18-0419

©2019 American Association for Cancer Research.

more pronounced immune alterations than transplanted cancer models (24), we investigated mice that develop endogenous lymphomas due to the presence of a *c-MYC* transgene specifically expressed in B cells (25). Using *MYC*-transgenic animals whose Foxp3^+ Tregs can be selectively depleted by diphtheria toxin (DT; refs. 5, 26), we show that Tregs contribute to tumor immune escape. In this model, we could identify specific self-peptides that are recognized by Tregs.

Materials and Methods

Animal experiments

All mice were kept in our animal facility under specific pathogen-free conditions. Experiments were performed in accordance with and with the approval of Regierung von Oberbayern. Mice were sacrificed when they had visible tumors. Spleens of treated animals were dissected for analyzing tumor-infiltrating immune cells and results were compared with untreated age-matched control mice.

Wild-type (WT) C57BL/6 mice were purchased from Taconic, λ -*MYC* C57BL/6 mice (25) were bred in our animal facility, DEREK mice were obtained from Technische Universität München and from The Jackson Laboratory. λ -*MYC*/DEREK mice were established by crossing DEREK mice with λ -*MYC* animals. Offspring carrying both the λ -*MYC* and the DEREK allele was identified using polymerase chain reaction (26). For specific depletion of Foxp3^+ Tregs, λ -*MYC*/DEREK mice were treated intraperitoneally (i.p.) with 0.5 μg DT (EMD Chemicals) per injection. Each depletion step required injections on two consecutive days (day 55/56, 69/70, and 83/84). The extent of depletion was confirmed on days 57, 71, and 85, respectively, by analyzing peripheral blood by flow cytometry using fluorochrome-labeled monoclonal antibodies (mAb) against *Foxp3*. A complete depletion was only seen after the first two treatment cycles, exactly as described earlier (26).

Flow cytometry

Mouse splenocytes were characterized by staining with fluorochrome-labeled mAbs against CD4 (RM4-5; eBioscience), CD69 (H1.2F3; eBioscience), CD62L (MEL-14; eBioscience), CTLA-4 (UC10-4B9; BioLegend), Neuropilin-1 (3E12; BioLegend), and CD137 (17B5; eBioscience) for 30 minutes at 4°C in FACS buffer. Occasionally, cells were also stained with LIVE/DEAD Fixable Blue Dead Cell Stain Kit (Thermo Fisher Scientific). Intracellular detection of *Foxp3*, Ki-67, and Helios was performed using the *Foxp3* Staining Kit with mAb against *Foxp3* (FJK-16s), Ki-67 (SolA15), and Helios (22F6, all eBioscience). For intracellular staining with mAbs to IL10 (JES5-16E3; eBioscience) and to IFN γ (XMG1.2, BioLegend), cells were stimulated for 4 hours with 1 $\mu\text{g}/\text{mL}$ PMA and 1 $\mu\text{g}/\text{mL}$ ionomycin (both Sigma-Aldrich) in the presence of 3 $\mu\text{g}/\text{mL}$ Brefeldin A (eBioscience). Cells were fixed with IC Fixation Buffer and permeabilized with 1 \times permeabilization buffer (both eBioscience) according to the manufacturer's protocol. Samples were measured on an LSR II flow cytometer (BD), and data were analyzed using the FlowJo software.

T-cell proliferation assay

Splenocytes from WT or λ -*MYC* mice were labeled with Cell Proliferation Dye (CPD) eFluor 450 (20 $\mu\text{mol}/\text{L}$; eBioscience) according to the manufacturer's protocol. A total of 0.5×10^6 cells

were seeded into each well of a 96-well U-bottom plate and stimulated with immobilized anti-CD3/anti-CD28 (2 $\mu\text{g}/\text{mL}$, Core Facility mAb, Helmholtz-Zentrum München) and rIL2 (50 U/mL) in RPMI-1640 medium (10% FCS). After 72 hours, cells were harvested, stained for CD4 and *Foxp3* and eFluor 450 dilution was analyzed by flow cytometry.

Cell culture

The murine B-cell lymphoma cell line 291 was derived from tumor-bearing λ -*MYC* mice in our own laboratory (27). The murine melanoma cell line B16F0 (28, 29) was obtained from ATCC in 2010 (ATCC; cat. # CRL-6322, RRID: CVCL_0604). All cells were kept in culture for no longer than 6 to 8 weeks. Cells were cultured in RPMI-1640 medium, supplemented with 5% fetal calf serum, penicillin (100 U/mL), streptomycin (100 $\mu\text{g}/\text{mL}$), 2 mmol/L L-glutamine, sodium pyruvate, nonessential amino acids, and 50 $\mu\text{mol}/\text{L}$ 2-mercaptoethanol (all from Thermo Fisher Scientific), at 37°C and 5% CO $_2$. MHC class II on 291 cells was induced by incubation with rIFN γ (10 4 U/mL) for 48 hours. Cell lines were regularly authenticated by virtue of *MYC* expression, cell morphology or growth behavior *in vitro* and *in vivo* and tested for *Mycoplasma* contamination before beginning of the experiments by using the Venor-GeM Classic kit (Minerva Biolabs, cat. # 11-1250).

Stimulation of T cells *in vitro*

CD4 $^+$ T cells from WT or λ -*MYC* spleens were obtained using the EasySep Mouse CD4 $^+$ T-Cell Isolation Kit (STEMCELL Technologies) according to the manufacturer's instructions. Sorted CD4 $^+$ cells were labeled with CPD, as described above, and stimulated (2 \times 10 5 /well) with irradiated (30 Gy) WT splenocytes (1.5 \times 10 5 /well) and rIL2 (50 U/mL) in the presence of irradiated (100 Gy) 291 or B16F0 cells (10 5 /well) in 96-well round-bottom plates. Alternatively, WT splenocytes were loaded with the indicated peptides (1 $\mu\text{g}/\text{mL}$; Metabion) for 2 hours at 37°C, washed and cocultured with sorted CD4 $^+$ T cells. Where indicated, anti-MHC-II (M5/114.15.2; eBioscience) was included (diluted 1:1,000). After 7 days, cells were harvested, stained with anti-*Foxp3* and anti-Ki-67 and analyzed by flow cytometry.

Identification of Treg epitopes

MHC class II ligands of λ -*MYC* lymphoma cells as well as WT cells were isolated by immunoaffinity chromatography. Cells were lysed in buffer containing PBS, 0.6% CHAPS, and complete protease inhibitor (Roche), shaken for 1 hour and subsequently sonicated for 1 minute. Following centrifugation for 1.5 hours, the supernatant was applied on affinity columns previously prepared by coupling anti-MHC II (M5/114.15.2; eBioscience) to CNBr-activated Sepharose (GE Healthcare; 1 mg mAb/40 mg Sepharose). Subsequently, columns were eluted using 0.2% trifluoroacetic acid (TFA). Filtration of the eluate through a 1 kDa filter (Merck Millipore) yielded the MHC class II ligands in solution. The filtrate was desalted with C $_{18}$ ZipTips (Merck Millipore) and subsequently concentrated using a vacuum centrifuge (Bachofer). Sample volume was adjusted for measurement by adding 1% AcN/0.05% TFA (v/v). With an injection volume of 5 μL , samples were loaded onto a precolumn (100 $\mu\text{m} \times 2 \text{ cm}$, C18, 5 μm , 100 Å) and separated on Acclaim Pepmap100 columns (75 $\mu\text{m} \times 50 \text{ cm}$, C18, 3 μm , 100 Å; Dionex) using an Ultimate 3000 RLSCnano uHPLC system (Dionex). A gradient

ranging from 2.4% to 32% of AcN/H₂O with 0.1% formic acid was used to elute the peptides from the columns over 125 minutes at a flow rate of 300 nL/min. Online electrospray ionization (ESI) was followed by tandem mass spectrometry (MS) analysis (30) in an LTQ Orbitrap XL instrument (Thermo Fisher Scientific). Survey

scans were acquired in the Orbitrap mass analyzer with a resolution of 60,000 and a mass range of 300 to 1500 m/z. Fragment mass spectra of the 5 most intense ions of each scan cycle were recorded in the linear ion trap (top5 CID). Normalized collision energy of 35%, activation time of 30 ms and isolation width of

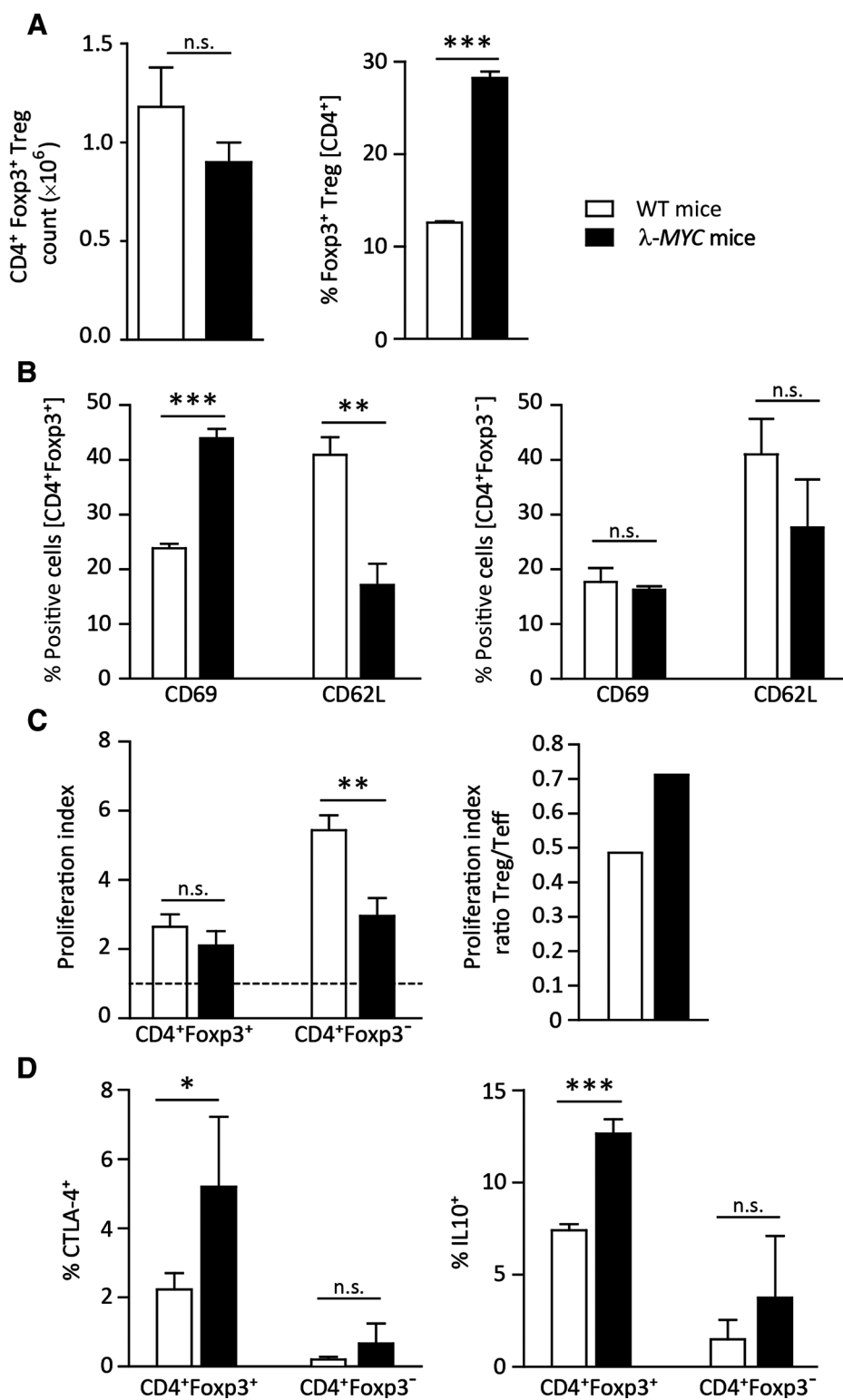


Figure 1.

Enhanced activation of CD4⁺Foxp3⁺ Tregs in spleens of tumor-bearing λ -MYC mice. **A**, Absolute numbers of Foxp3⁺ Tregs in spleens of diseased λ -MYC mice ($n = 20$) and WT mice ($n = 42$; left) and fraction of Foxp3⁺ Tregs within the CD4⁺ T-cell compartments (right). All animals had identical tumor burdens, because analyses had to be done when clinical symptoms became visible. At earlier time points, tumor loads cannot be quantitated (see Results section). The animals analyzed had an age of 80 to 120 days. **B**, Enhanced activation of intratumoral Foxp3⁺ Tregs (left), shown by an increase of the early activation marker CD69 ($n = 10$) and a decrease of CD62L ($n = 5$) compared with WT splenocytes ($n = 20$ and $n = 4$). For comparison, the activation markers of Foxp3⁻ cells are also shown (right). **C**, Left, proliferation indices of Foxp3⁺ Treg and Foxp3⁻ Teff cells from λ -MYC spleens ($n = 12$) in comparison with WT mice ($n = 20$). Proliferation was measured after stimulation with anti-CD3/anti-CD28 *in vitro* and normalized to unstimulated control splenocytes from WT mice (proliferation index = 1; broken line). Right, ratio of the mean Treg to Teff proliferation indices in λ -MYC animals compared with WT mice. **D**, Compiled data on CTLA-4 and IL10 expression in CD4⁺Foxp3⁺ Tregs of diseased λ -MYC mice ($n = 6$ and $n = 16$) compared with WT mice ($n = 13$ and $n = 12$). For CTLA-4, surface expression is shown because this is relevant for potential suppressor activity mediated by cell contact. The expression patterns of Foxp3⁻ cells are included for comparison.

2 m/z was utilized for fragment mass analysis. Dynamic exclusion was set to 1 second. The RAW files were processed against the murine proteome as comprised in the Swiss-Prot database using MASCOT server version 2.3.04 (Matrix Science) and Proteome Discoverer 1.4 (Thermo Fisher Scientific). A mass tolerance of 5 ppm or 0.5 Da was allowed for parent and fragment masses, respectively. Filtering parameters were set to a Mascot Score < 20, search engine rank = 1, peptide length of 15 to 25 AA, achieving a false discovery rate of 5% as determined by an inverse decoy database search.

Quantitative reverse-transcription polymerase chain reaction (qRT-PCR)

A total of 10^6 291, B16F0, or immunomagnetically separated WT B cells were lysed in 200 μ L TRIzol reagent (Invitrogen). Then, total RNA was extracted with 1-Bromo-3-chloro-propane (Sigma) followed by precipitation with isopropanol. cDNA was generated by reverse transcription using the First-Strand cDNA Synthesis kit (Roche Diagnostics) and quantified with primer pairs (Metabion) specific for the genes that had been identified on the basis of peptide-specific T-cell stimulation. Expression of the 18s gene was used as a reference. After amplification in a LightCycler 2.0 Real-Time PCR system (Roche Diagnostics), the specific signals were normalized to those obtained for 18s and for WT B cells.

Statistical analysis

Data analysis was performed using Prism 5.0 software (GraphPad). All results were expressed as means \pm SEM. A normal distribution was assumed for the experiments, and all data were subjected to the Grubbs test for statistical outliers. The unpaired Student *t* test was used to assess differences between two independent groups. Survival curves of λ -MYC/DEREG mice were compared using the log-rank (Mantel-Cox) test. Unless otherwise indicated, *n* refers to the number of mice or samples from different mice. The significance level is depicted as follows: *, *P* < 0.05; **, *P* < 0.01; and ***, *P* < 0.001.

Results

Lymphoma-infiltrated spleens harbor activated and proliferating Foxp3⁺ Tregs

λ -MYC mice bear the *MYC* oncogene under the control of the B-cell-specific immunoglobulin λ enhancer and develop clinically apparent lymphomas at an age of about 80 to 120 days. Tumors grow in spleens and lymph nodes and reflect several biological features of human Burkitt lymphoma (25). The mice are euthanized as soon as clinical symptoms become visible; at these time points, the tumor loads are identical. In earlier disease phases, tumor burdens cannot be quantitated because normal and malignant B cells cannot be discriminated.

To address the role of Tregs in this endogenous lymphoma model, we initially examined the frequency of CD4⁺ Foxp3⁺ T cells in tumor-infiltrated spleens of diseased λ -MYC mice. In comparison with normal spleens, the absolute numbers of Foxp3⁺ cells were diminished, but their fraction within the CD4⁺ population, hence the ratio between Foxp3⁺ and Foxp3⁻ cells, was significantly augmented in the lymphomas (Fig. 1A). Further analyses of the CD4⁺ Foxp3⁺ Treg population in tumors revealed an activated phenotype that was evident by the upregulation of the early activation marker CD69 and downregulation of L-selectin CD62L (Fig. 1B).

The increased ratio of Treg to Teff cells in spleens of tumor-bearing mice might be ascribed to differential proliferation of the two T-cell subtypes. Therefore, we determined the numbers of cycling cells after CD3 and CD28 stimulation *in vitro*. Both CD4⁺ Foxp3⁻ Teff and CD4⁺ Foxp3⁺ Tregs showed decreased expansion *in vitro* as compared with healthy WT mice, which might indicate a state of exhaustion following chronic stimulation *in vivo*. However, this impairment was significant in the Teff cell compartment only (Fig. 1C). The differential suppression of proliferation may explain the increased fraction of Tregs within the CD4⁺ compartment of λ -MYC spleens.

We then examined the expression of molecules that may impart immunosuppressive functions of the Tregs. Compared with its WT counterpart, the Foxp3⁺ Treg compartment of tumor mice showed higher fractions of cells expressing IL10 and CTLA-4, respectively (Fig. 1D). As expected, no expression of interferon- γ (IFN γ) was detected in the Tregs.

Lymphoma growth is suppressed in the absence of Foxp3⁺ Tregs

To elucidate the functional relevance of the Tregs found in endogenous lymphoma, we crossed λ -MYC animals with DEREK mice, which are engineered to express a fusion gene encoding the DT receptor and the green fluorescent protein under the control of the Foxp3 locus. DT treatment of DEREK animals resulted in a selective ablation of the Foxp3⁺ Treg compartment (Fig. 2A), as described earlier (5, 26).

If untreated, the λ -MYC/DEREG strain developed lymphomas with the same kinetics as the parental λ -MYC mice. However, when these λ -MYC/DEREG animals were depleted of Foxp3⁺ Tregs by injecting DT between days 55 and 84 after birth (26), a significant delay of tumor growth was observed (Fig. 2B). When spleens of DT-injected λ -MYC/DEREG mice were isolated, an elevated fraction of CD8⁺ T cells, but not other immune cells,

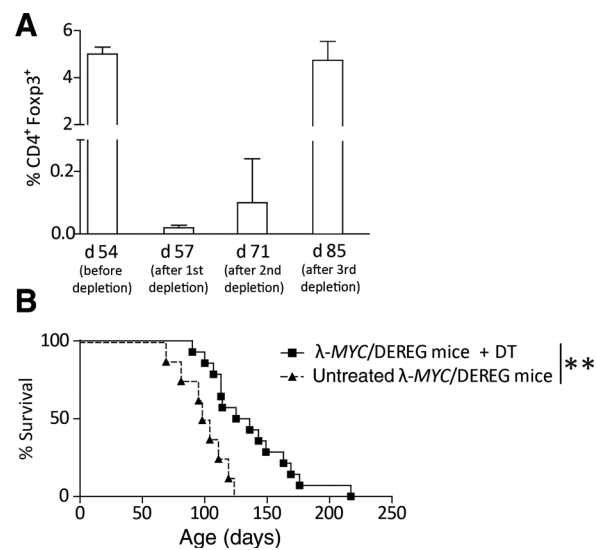


Figure 2. Treg depletion in λ -MYC/DEREG mice induces prolonged survival. **A**, Effect of DT injection on CD4⁺ Foxp3⁺ T-cell counts in peripheral blood (*n* = 4). **B**, Kaplan-Meier diagram showing the survival times of λ -MYC/DEREG mice treated with DT (*n* = 14) compared with untreated controls (*n* = 8).

was found in comparison with untreated λ -MYC/DEREG animals (Supplementary Fig. S1). Thus, the effector cells that benefit from Treg depletion may mainly be $CD8^+$ T cells, as described earlier (19). Taken together, our results strongly suggest that $Foxp3^+$ Tregs suppress immune responses against endogenous lymphoma.

Tregs in λ -MYC lymphoma are predominantly nTregs

To shed light on the origin of the Treg fraction in λ -MYC tumors, we analyzed the expression of the transcription factor Helios, a member of the Ikaros family, and the surface protein Nrp-1. Most intratumoral $Foxp3^+$ Tregs were $Helios^+$ and $Nrp-1^+$ (Fig. 3A and B). This phenotype indicates that the majority of the $Foxp3^+$ Tregs in tumor spleens are nTregs. Because the

proportion of $Foxp3$ positivity within the $CD4^+$ population rose by a factor of 2.3 after tumor development (Fig. 1A) and the percentage of $Helios^+$ cells within the $Foxp3^+$ compartment increased only 1.3-fold (Fig. 3A), a slight increment of $Helios^-$ Tregs within the total $CD4^+$ population has also occurred (Fig. 3C). $Helios^+$ cells showed a significantly higher amount of the proliferation marker Ki-67 compared with the $Helios^-$ population (Fig. 3D) and expressed significantly more CD137 than their $Helios^-$ counterparts (Fig. 3E). This molecule, which is a marker of effector T cells with known and unknown antigen reactivity, was mostly confined to the $Helios^+$ subpopulation (Fig. 3F). Taken together, the data suggest that immunosuppressive $Foxp3^+$ Tregs in λ -MYC lymphomas are predominantly derived from the nTreg compartment.

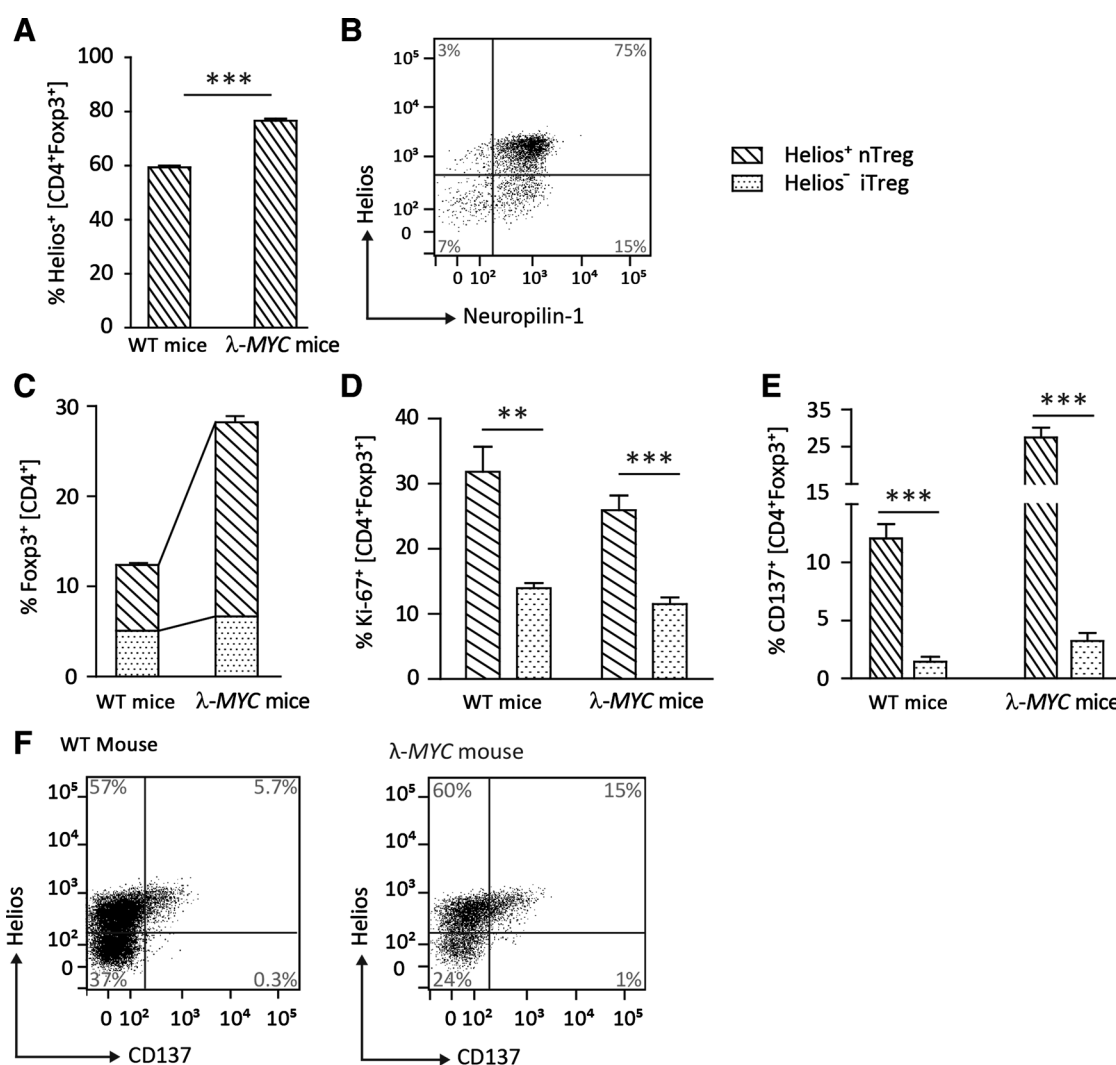
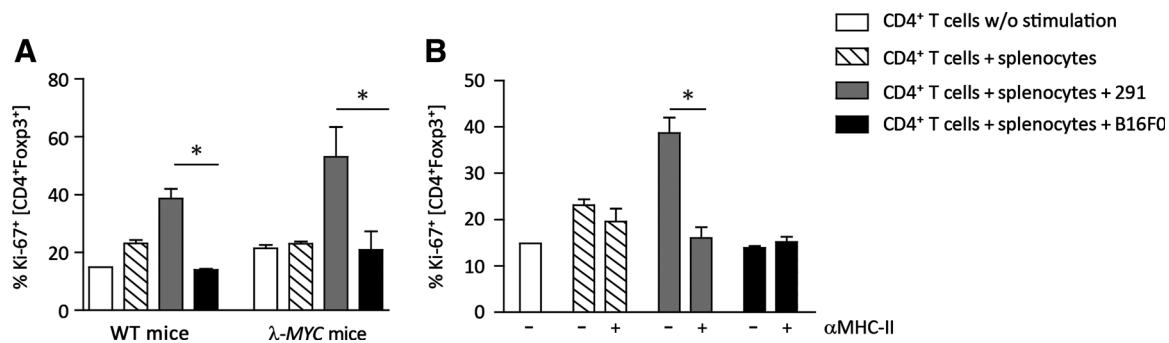


Figure 3.

$Foxp3^+$ nTregs play a role in λ -MYC tumors. **A**, Increased fraction of $Helios^+$ cells in the $CD4^+Foxp3^+$ compartment of tumor-bearing λ -MYC mice ($n = 23$) compared with WT mice ($n = 18$). **B**, Representative diagram showing the coexpression of Helios and Nrp-1 in $CD4^+Foxp3^+$ Tregs from a diseased λ -MYC mouse. **C**, Distribution of $Helios^+$ and $Helios^-$ cells within the total $CD4^+$ population of WT ($n = 18$) and λ -MYC mice ($n = 23$). **D**, Enhanced proliferation of intratumoral $Foxp3^+Helios^+$ compared with $Foxp3^+Helios^-$ Tregs from λ -MYC mice ($n = 6$) compared with WT mice ($n = 5$). **E**, Expression of CD137 on $Helios^+$ and $Helios^-$ Tregs from λ -MYC mice ($n = 6$) compared with WT spleens ($n = 5$). **F**, Coexpression of Helios and CD137 in $Foxp3^+$ Tregs. Representative dot plot from six and five experiments, respectively.

**Figure 4.**

Response of Foxp3⁺ Tregs to lymphoma-associated antigens. **A**, Proliferation of Foxp3⁺ Tregs from up to four WT and λ-MYC mice after *in vitro* stimulation of sorted CD4⁺ cells with irradiated WT splenocytes and 291 or B16F0 cells for 7 days. Foxp3⁻ cells showed the same response pattern to these stimulators, although the Ki-67 percentages were somewhat lower than in Foxp3⁺ cells (shown for splenocytes and 291 cells + splenocytes, respectively, in Fig. 5B). **B**, Proliferation of WT Foxp3⁺ Tregs in the presence or absence of an MHC II-blocking antibody (*n* = 3).

Foxp3⁺ Tregs in lymphoma recognize specific peptides

In light of these results, we speculated that the Foxp3⁺ Tregs identified in λ-MYC mice recognize specific tumor-associated self-peptides via their TCR. To test this hypothesis, we cocultivated total purified CD4⁺ T cells from tumor-bearing λ-MYC mice with irradiated tumor cells. As specific stimulators, we used 291 cells, which were derived from a λ-MYC tumor (27). The B16F0 melanoma served as an irrelevant control tumor.

When Ki-67 was analyzed in the gate of the CD4⁺ Foxp3⁺ population after 7 days, an augmented activation status of the Tregs was found after their stimulation in the presence of the MYC lymphoma but not in the presence of the control cells. The same results were obtained when the T cells were derived from healthy WT mice (Fig. 4A). We therefore hypothesized that the peptides interacting with Tregs of λ-MYC as well as WT mice represent normal self-antigens, which may be overexpressed in the lymphoma cells.

To define these self-peptides, we first asked whether lymphoma recognition by Foxp3⁺ Tregs is MHC class II restricted. Indeed, the lymphoma-dependent Treg stimulation observed could be abrogated by mAb-mediated blockade of MHC class II during cocultivation (Fig. 4B). This prompted us to isolate MHC class II-peptide complexes from λ-MYC lymphoma as well as from normal WT cells by affinity chromatography using anti-MHC II. Peptides were eluted and subsequently subjected to MS, as outlined in Materials and Methods. Sixty-eight sequences were identified after elution from the λ-MYC cells, which were prevalent in the lymphoma as compared with normal B cells and which could

be assigned to a total of 44 proteins (Supplementary Table S1). From those proteins, 10 were selected on the basis of their potential involvement in processes such as cell-cycle control, apoptosis, or malignant transformation. Based on the core sequences revealed by MS, 10 synthetic peptides were then generated representing each of the proteins (Table 1).

These synthetic peptides were examined with respect to their capability of stimulating the proliferation of Foxp3⁺ Tregs. To this end, normal splenocytes were pulsed with the synthetic peptides and cultivated together with CD4⁺ T cells from λ-MYC mice. Then, proliferation was measured in the Foxp3⁺ as well as the Foxp3⁻ fraction. Four of the 10 peptides were able to induce proliferative responses of the Foxp3⁺ Tregs that were significantly different from those Treg responses that were seen after incubation with normal B cells and antigen-presenting cells in the absence of peptides (Fig. 5A). This peptide reactivity was evident mainly in the Helios⁺ nTreg but not in the Helios⁻ iTreg population (Supplementary Fig. S2A). As expected, the T-cell responses that were significantly different from the control could be abolished by blocking MHC II (Supplementary Fig. S2B). The identified peptide sequences originated from gene loci that are related to silencing of tumor suppressor genes, regulating cell growth and promoting metastasis. A similar stimulation pattern was detected in the Foxp3⁻ Teff fraction (Fig. 5B), indicating that potentially protective Teff cells may be suppressed by Tregs directed against the same epitopes.

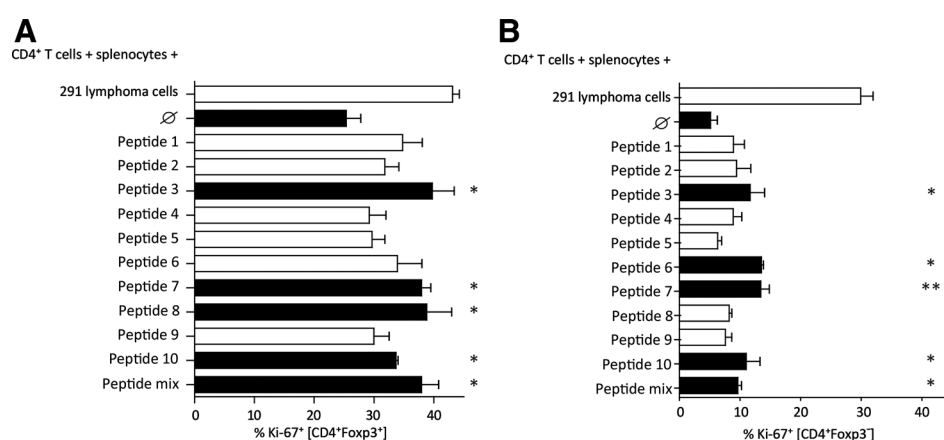
To determine whether these peptides may be overexpressed in lymphoma cells, we examined the expression of peptides, which

Table 1. Peptides selected for T-cell stimulation *in vitro*

Peptide	Peptide sequence	Gene	Protein
1	GSPVIAAANSLGIPVAAAAGAQQ	Csnk2a1	Casein kinase II subunit alpha
2	DLDAPDDVDF	Srrt	Serrate RNA effector molecule homolog
3	LERLDLDTSDSQPPVF	Trim28	Transcription intermediary factor 1-beta
4	DSWIVPLDNLTKDDLDEEEDTHL	Podxl	Podocalyxin
5	APIDRVGTIE	Hnrnpm	Heterogeneous nuclear ribonucleoprotein M
6	EALEQGILP	Cdk7	Cyclin-dependent kinase 7
7	VRPPVPLPASSHPASTNEPIVLED	Mta2	Metastasis-associated protein MTA2
8	EAVLTGLVEA	Telo2	Telomere length regulation protein TEL2 homolog
9	SIAAFIQRL	Bag6	Large proline-rich protein BAG6
10	RIEPLSPSKN	Fxyd5	FXD domain-containing ion transport regulator 5

NOTE: Based on the core sequences identified by MS (see text), 10 synthetic peptides were synthesized and used for *in vitro* T-cell stimulation assays.

Ahmetlić et al.

**Figure 5.**

In vitro stimulation of Tregs by 10 selected peptides. As in Fig. 4A, sorted CD4⁺ T cells were stimulated *in vitro* with irradiated WT splenocytes and 291 cells as a positive control. Alternatively, cocultures were performed using irradiated WT splenocytes that had been pulsed before with the synthetic peptides shown in Table 1. **A**, Proliferation of the Foxp3⁺ Tregs in different cocultures was measured by flow cytometry on day 7 and compared with the negative control with peptides or 291 cells. Only four peptides and a mix of all peptides yielded Ki-67 levels that were significantly different from the negative control (denoted by black bars and asterisks). Identical recognition patterns emerged when T cells from tumor and healthy animals, respectively, were used. **B**, Analysis of the Foxp3⁻ Teff cell fraction revealed a similar recognition pattern as found for Foxp3⁺ cells (with the exception of peptide 8). The differences between Tregs and Teffs with regard to the proliferation induced were statistically significant for each single peptide. In both **A** and **B**, the differential ability of peptides to significantly stimulate T cells suggests that T-cell responses—if they occur—are antigen dependent. The same results were obtained by measuring CPD dilution in stimulated T cells. Each bar represents the mean from four independent experiments.

did or did not stimulate Tregs, by qRT-PCR. Recognition by T cells always correlated with increased expression of the corresponding genes in 291 versus control tumor cells (Supplementary Fig. S3). The results for genes that encode peptides not recognized by T cells, however, were less consistent. Indeed, high expression in 291 cells did not necessarily predict efficient peptide presentation (as observed for peptide 4).

Discussion

For developing approaches to cancer treatment, we must understand the pathways of tumor immune escape. We investigated a lymphoma model because therapy of this disorder in the clinics demands further improvement. In the λ -MYC transgenic endogenous tumor model, numerous alterations have been identified that allow protective antitumor immune responses to be overridden. Thus, natural killer cells, T cells, and dendritic cells become impaired during lymphoma growth, and a tumor-promoting microenvironment is created, which, e.g., involves the cytokine milieu (24, 27, 31–33).

Here, we show that Foxp3⁺ Tregs mediate immune escape in endogenous B-cell lymphoma, because tumor development was delayed after DT-mediated ablation of Foxp3⁺ Tregs in λ -MYC/DEREG mice. Tregs recover about 2 weeks following initial depletion in DEREG mice (26, 34). In our model, depletion started at day 55 after birth, a time point when malignant cells were presumably already present, albeit clinically still unapparent (27). The second depletion cycle at days 69 and 70 was as successful as the first one. A third DT treatment cycle at days 83/84 was no longer effective, perhaps due to loss of the transgene and/or induction of a humoral anti-DT response (26, 34). Therefore, the antitumor effect induced by depletion of Foxp3⁺ Tregs in the λ -MYC model may even be underestimated. At the time points

when mice were sacrificed, the tumor loads were identical irrespective of whether or not Tregs had been depleted. Thus, the survival benefit effected by Treg depletion is only the result of a delay of tumor growth in early disease phases, which, however, cannot be monitored in the λ -MYC model because normal and malignant B cells cannot be discriminated. A tumor-promoting role of Tregs was also described in other lymphoma models (35–37), but these studies were only done using transplanted tumors, which do not reflect the tumor-induced immune alterations as closely as our clinically relevant endogenous lymphoma model (24, 27).

The Treg-to-Teff ratio was elevated in tumor-infiltrated spleens of λ -MYC mice, which could be explained by a differential suppression of the proliferation of the two T-cell subsets. Of course, an unequal recruitment into the growing tumor as an additional mechanism cannot be precluded. The upregulation of CD69 on intratumoral Tregs indicates immunosuppressive activity (38) but might also reflect retention of the cells (39). Activation of Tregs associated with CD69 upregulation was also observed in a model of carcinogen-induced fibrosarcoma where thymus-derived Helios-expressing Tregs accumulated in the tumor tissue and showed increased proliferation as indicated by their expression of Ki-67 (40).

A central question pertains to the identity and Ag specificity of Tregs. In infectious disease of the central nervous system, for example, virus-specific Tregs seem to arise from the nTreg compartment and suppress Teffs upon interaction with cognate virus epitopes (41). Immunosuppressive nTregs recognizing specific peptides may also play a role in limiting proinflammatory responses against cancer. MHC class II-restricted self-peptides that are recognized by a Treg clone are prevalent in mouse prostate carcinoma, thus indicating that these Tregs are thymus-derived nTregs (42).

In line with these results, we mainly found thymus-differentiated nTregs in the B-cell lymphomas. A slight—albeit not statistically significant—increase of iTregs, which, in contrast to nTregs, arise from Teffs converted in the periphery to express Foxp3, was also observed. Given the role of TCR-dependent recognition of self-peptide–MHC class II complexes for driving nTreg development in the thymus (20, 43) and for subsequent induction of immune tolerance in the periphery, it was of interest to define the peptides recognized by Tregs in B-cell lymphoma. The pattern of recognition of tumor cells by Tregs suggested that the specificities involved are not only present in tumor-bearing but also in healthy WT mice. The sequences that stimulated Tregs were indeed nonmutated self-epitopes, which also occurred in WT cells. Thus, the responses observed were not dependent on the origin of the Tregs but presumably just on altered presentation of the (normal) peptides by the tumor. The epitopes originated from proteins whose functions are, among others, related to malignant transformation. These proteins were overexpressed in the lymphoma cells but not in the control tumor. However, genes were also identified that are overexpressed in 291 cells, even though their products are not recognized by Tregs. Indeed, high gene expression does not necessarily give rise to efficient peptide presentation.

The mode of action of Tregs in λ -MYC tumor mice has not yet been elucidated in detail. In previous studies, suppression of Teff cells mediated by IL10 or TGF β or by IL2 deprivation as well as a cytotoxic activity against antigen-presenting cells was postulated (44–46). In particular, it is not yet clear by which mechanisms the peptide-specific Treg activation leads to Teff cell suppression in the λ -MYC model. Experiments suggest that Tregs from MYC mice exert suppressor activity, which is partly dependent on IL10, and that peptide recognition by Tregs correlates with their IL10 expression. However, cellular contacts may also play a role. Of course, the increased ratio of Tregs-to-Teffs in tumor spleens should be relevant for Treg-induced diminution of antitumor responses.

The pattern of peptide recognition was similar when Treg and Teffs were compared. With the exception of peptide 8, all epitopes recognized by Tregs were also able to induce statistically significant proliferation of Teffs. This suggests that Tregs may be recruited selectively against tumor antigens that could serve as targets for potentially protective Teffs.

Even more Treg specificities may exist in λ -MYC tumors in addition to the four epitopes described in this paper, because only

10 antigens were selected for detailed analysis of their potential to stimulate Tregs. Nonetheless, the data presented here demonstrate the principle that lymphomas may use Tregs to counteract the attack of immune effector cells.

Disclosure of Potential Conflicts of Interest

M. Röcken discloses professional relationships with Deutsche Dermatologische Gesellschaft, Deutsche Forschungsgemeinschaft, Deutsche Krebshilfe, European Academy of Dermatology and Venereology, Institut für medizinische und pharmazeutische Prüfungsfragen, and Wilhelm Sander-Stiftung; is responsible for study recruitment for AB Science, Abbott Laboratories, Abbott Pharmaceuticals, Abbvie Deutschland, Almirall Hermal, Astra Zeneca, Bayer, Biogen, Bristol-Myers Squibb, Celgene, Galderma, and GSK; and is a shareholder or patent holder for Merck & Company, MSD Sharp & Dohme, and EP-Patent 13826993.1. No potential conflicts of interest were disclosed by the other authors.

Authors' Contributions

Conception and design: M. Röcken, R. Mocikat

Development of methodology: F. Ahmetlić, T. Riedel

Acquisition of data (provided animals, acquired and managed patients, provided facilities, etc.): F. Ahmetlić, N. Hömberg, V. Bauer, N. Trautwein, A. Geishauser, S. Stevanović

Analysis and interpretation of data (e.g., statistical analysis, biostatistics, computational analysis): F. Ahmetlić, T. Riedel, N. Hömberg, V. Bauer, S. Stevanović, M. Röcken, R. Mocikat

Writing, review, and/or revision of the manuscript: F. Ahmetlić, T. Riedel, M. Röcken, R. Mocikat

Administrative, technical, or material support (i.e., reporting or organizing data, constructing databases): A. Geishauser, T. Sparwasser

Study supervision: R. Mocikat

Acknowledgments

The work was supported by grants from Deutsche Krebshilfe (70112332, 70112337, 110662, and 110664), Wilhelm-Sander-Stiftung (2012.056.3), and Deutsche Forschungsgemeinschaft (SFB-TR 156).

We are grateful to Michael Hagemann, Franziska Liebel, and Jasmin Teutsch for taking care of animal husbandry and Angela Hoffmann for help in preparing the manuscript. The study includes parts of the doctoral theses of F.A. and T.R. at the Ludwig-Maximilians-Universität München.

The costs of publication of this article were defrayed in part by the payment of page charges. This article must therefore be hereby marked *advertisement* in accordance with 18 U.S.C. Section 1734 solely to indicate this fact.

Received June 21, 2018; revised November 13, 2018; accepted January 29, 2019; published first March 20, 2019.

References

- Wing K, Sakaguchi S. Regulatory T cells exert checks and balances on self tolerance and autoimmunity. *Nat Immunol* 2010;11:7–13.
- Vignali DA, Collison LW, Workman CJ. How regulatory T cells work. *Nat Rev Immunol* 2008;8:523–32.
- Zheng Y, Rudensky AY. Foxp3 in control of the regulatory T cell lineage. *Nat Immunol* 2007;8:457–62.
- Sakaguchi S. Naturally arising Foxp3-expressing CD25⁺CD4⁺ regulatory T cells in immunological tolerance to self and non-self. *Nat Immunol* 2005;6:345–52.
- Lahl K, Loddenkemper C, Drouin C, Freyer J, Arnason J, Eberl G, et al. Selective depletion of Foxp3⁺ regulatory T cells induces a scurfy-like disease. *J Exp Med* 2007;204:57–63.
- Fatini MC, Becker C, Monteleone G, Pallone F, Galle PR, Neurath MF. Cutting edge: TGF-beta induces a regulatory phenotype in CD4⁺. *J Immunol* 2004;172:5149–53.
- Fontenot JD, Rasmussen JP, Williams LM, Dooley JL, Farr AG, Rudensky AY. Regulatory T cell lineage specification by the forkhead transcription factor Foxp3. *Immunity* 2005;22:329–41.
- Curotto de Lafaille MA, Lafaille JJ. Natural and adaptive foxp3⁺ regulatory T cells: more of the same or a division of labor? *Immunity* 2009;30:626–35.
- Thornton AM, Korty PE, Tran DQ, Wohlfert EA, Murray PE, Belkaid Y, et al. Expression of Helios, an Ikaros transcription factor family member, differentiates thymic-derived from peripherally induced Foxp3⁺ T regulatory cells. *J Immunol* 2010;184:3433–41.
- Akimova T, Beier UH, Wang L, Levine MH, Hancock WW. Helios expression is a marker of T cell activation and proliferation. *PLoS One* 2011;6:e24226.
- Serre K, Benezec C, Desanti G, Bobat S, Toellner KM, Bird R, et al. Helios is associated with CD4 T cells differentiating to T helper 2 and follicular helper T cells in vivo independently of Foxp3 expression. *PLoS One* 2011;6:e20731.

12. Gottschalk RA, Corse E, Allison JP. Expression of Helios in peripherally induced Foxp3⁺ regulatory T cells. *J Immunol* 2012;188:976–80.
13. Yadav M, Louvet C, Davini D, Gardner JM, Martinez-Llordella M, Bailey-Bucktrout S, et al. Neuropilin-1 distinguishes natural and inducible regulatory T cells among regulatory T cell subsets in vivo. *J Exp Med* 2012;209:1713–22.
14. Weiss JM, Bilate AM, Gobert M, Ding Y, Curotto de Lafaille MA, Parkhurst CN, et al. Neuropilin-1 is expressed on thymus-derived natural regulatory T cells, but not mucosa-generated induced Foxp3⁺ Treg cells. *J Exp Med* 2012;209:1723–42.
15. Wolf D, Wolf AM, Rumpold H, Fiegl H, Zeimet AG, Muller-Holzner E, et al. The expression of the regulatory T cell-specific forkhead box transcription factor FoxP3 is associated with poor prognosis in ovarian cancer. *Clin Cancer Res* 2005;11:8326–31.
16. Clarke SL, Betts GJ, Plant A, Wright KL, El-Shanawany TM, Harrop R, et al. CD4⁺CD25⁺FOXP3⁺ regulatory T cells suppress anti-tumor immune responses in patients with colorectal cancer. *PLoS One* 2006;1:e129.
17. Facciabene A, Motz GT, Coukos G. T-regulatory cells: key players in tumor immune escape and angiogenesis. *Cancer Res* 2012;72:2162–71.
18. Bos PD, Plitas G, Rudra D, Lee SY, Rudensky AY. Transient regulatory T cell ablation deters oncogene-driven breast cancer and enhances radiotherapy. *J Exp Med* 2013;210:2435–66.
19. Klages K, Mayer CT, Lahl K, Loddenkemper C, Teng MWL, Foong Ngiew S, et al. Selective depletion of Foxp3⁺ regulatory T cells improves effective therapeutic vaccination against established melanoma. *Cancer Res* 2010;70:7788–99.
20. Hsieh CS, Liang Y, Tzysnik AJ, Self SG, Liggitt D, Rudensky AY. Recognition of the peripheral self by naturally arising CD25⁺ CD4⁺ T cell receptors. *Immunity* 2004;21:267–77.
21. Lathrop SK, Santacruz NA, Pham D, Luo J, Hsieh CS. Antigen-specific peripheral shaping of the natural regulatory T cell population. *J Exp Med* 2008;205:3105–17.
22. Fisson S, Darrasse-Jeze G, Litvinova E, Septier F, Klatzmann D, Liblau R, et al. Continuous activation of autoreactive CD4⁺CD25⁺ regulatory T cells in the steady state. *J Exp Med* 2003;198:737–46.
23. Moran AE, Holzapfel KL, Xing Y, Cunningham NR, Maltzman JS, Punt J, et al. T cell receptor signal strength in Treg and iNKT cell development demonstrated by a novel fluorescent reporter mouse. *J Exp Med* 2011;208:1279–89.
24. Przewoznik M, Hömberg N, Naujoks M, Pötzl J, Münchmeier N, Brenner C, et al. Recruitment of natural killer cells in advanced stages of endogenously arising B-cell lymphoma: Implications for therapeutic cell transfer. *J Immunother* 2012;35:217–22.
25. Kovalchuk AL, Qi C-F, Torrey TA, Taddesse-Heath L, Feigenbaum L, Sup Park S, et al. Burkitt lymphoma in the mouse. *J Exp Med* 2000;192:1183–90.
26. Lahl K, Sparwasser T. In vivo depletion of FoxP3 Tregs using the DEREK mouse model. In: Kassiotis G, Liston A, editors. *Regulatory T cells: Methods and protocols. Methods in Molecular Biology. Vol. 707. Switzerland: Springer; 2011:157–72.*
27. Brenner C, King S, Przewoznik M, Wolters I, Adam C, Bornkamm G, et al. Requirements for control of B-cell lymphoma by NK cells. *Eur J Immunol* 2010;40:494–504.
28. Fidler IJ. Biological behavior of malignant melanoma cells correlated to their survival in vivo. *Cancer Res* 1975;35:218–24.
29. Nicolson GL, Brunson KW, Fidler IJ. Specificity of arrest, survival, and growth of selected metastatic variant cell lines. *Cancer Res* 1978;38:4105–11.
30. Dongre AR, Kovats S, deRoos P, McCormack AL, Nakagawa T, Paharkova-Vatchkova V, et al. In vivo MHC class II presentation of cytosolic proteins revealed by rapid automated tandem mass spectrometry and functional analyses. *Eur J Immunol* 2001;31:1485–94.
31. Naujoks M, Weiß J, Riedel T, Hömberg N, Przewoznik M, Nößner E, et al. Alterations of costimulatory molecules and instructive cytokines expressed by dendritic cells in the microenvironment of an endogenous mouse lymphoma. *Cancer Immunol Immunother* 2014;63:491–9.
32. Belting L, Hömberg N, Przewoznik M, Brenner C, Riedel T, Flatley A, et al. Critical role of the NKG2D receptor for NK cell-mediated control and immune escape of B-cell lymphoma. *Eur J Immunol* 2015;45:2593–601.
33. Pötzl J, Roser D, Bankel L, Hömberg N, Geishauer A, Brenner C, et al. Reversal of tumor acidosis by systemic buffering reactivates NK cells to express IFN- γ and induces NK cell-dependent lymphoma control without other immunotherapies. *Int J Cancer* 2017;140:2125–33.
34. Riedel T. Intratumorale T-Zellen in einem Spontanlymphommodell der Maus: Aktivierende und supprimierende Mechanismen. Dissertation, Ludwig-Maximilians-Universität München; 2013.
35. Elpek KG, Lacelle C, Singh NP, Yolcu ES, Shirwan H. CD4⁺CD25⁺ T regulatory cells dominate multiple immune evasion mechanisms in early but not late phases of tumor development in a B cell lymphoma model. *J Immunol* 2007;178:6840–8.
36. Deligne C, Metidji A, Fridman W-H, Teillaud J-L. Anti-CD20 therapy induces a memory Th1 response through the IFN- γ /IL-12 axis and prevents protumor regulatory T-cell expansion in mice. *Leukemia* 2015;29:947–57.
37. Houot R, Goldstein MJ, Kohrt HE, Myklebust JH, Alizadeh AA, Lin JT, et al. Therapeutic effect of CD137 immunomodulation in lymphoma and its enhancement by T_{reg} depletion. *Blood* 2009;114:3431–8.
38. Cortés JR, Sánchez-Díaz R, Bovolenta ER, Barreiro O, Lasarte S, Matesanz Marín A, et al. Maintenance of immune tolerance by Foxp3⁺ regulatory T cells requires CD69 expression. *J Autoimmunity* 2014;55:51–62.
39. Mackay LK, Braun A, Macleod BL, Collins N, Tebartz C, Bedoui S, et al. CD69 interference with sphingosine-1-phosphate receptor function regulates peripheral T cell retention. *J Immunol* 2015;194:2059–63.
40. Colbeck EJ, Hindley JP, Smart K, Jones E, Bloom A, Bridgeman H, et al. Eliminating roles for T-bet and IL2 but revealing superior activation and proliferation as mechanisms underpinning dominance of regulatory T cells in tumors. *Oncotarget* 2015;6:24649–59.
41. Zhao J, Zhao J, Fett C, Trandem K, Fleming E, Perlman S. IFN- γ - and IL-10-expressing virus epitope-specific Foxp3⁺ Treg cell in the central nervous system during encephalomyelitis. *J Exp Med* 2011;208:1571–7.
42. Leonard JD, Gilmore DC, Dileepan T, Nawrocka WI, Chao JL, Schoenbach MH, et al. Identification of natural regulatory T cell epitopes reveals convergence on a dominant autoantigen. *Immunity* 2017;47:107–17.
43. Hsieh CS, Lee HM, Lio CW. Selection of regulatory T cells in the thymus. *Nat Rev Immunol* 2012;12:157–67.
44. Chen ML, Pittet MJ, Gorelik L, Flavell RA, Weissleder R, von Boehmer H, et al. Regulatory T cells suppress tumor-specific CD8 T cell cytotoxicity through TGF- β signals in vivo. *Proc Natl Acad Sci USA* 2005;102:419–24.
45. Boissonnas A, Scholer-Dahirel A, Simon-Blancal V, Pace L, Valet F, Kissenpfennig A, et al. Foxp3⁺ T cells induce perforin-dependent dendritic cell death in tumor-draining lymph nodes. *Immunity* 2010;32:266–78.
46. Pandiyan P, Zheng L, Ishihara S, Reed J, Lenardo MJ. CD4⁺CD25⁺Foxp3⁺ regulatory T cells induce cytokine deprivation-mediated apoptosis of effector CD4⁺ T cells. *Nat Immunol* 2007;8:1353–62.

Cancer Immunology Research

Regulatory T Cells in an Endogenous Mouse Lymphoma Recognize Specific Antigen Peptides and Contribute to Immune Escape

Fatima Ahmetlic, Tanja Riedel, Nadine Hömberg, et al.

Cancer Immunol Res 2019;7:600-608. Published OnlineFirst March 20, 2019.

Updated version Access the most recent version of this article at:
doi:[10.1158/2326-6066.CIR-18-0419](https://doi.org/10.1158/2326-6066.CIR-18-0419)

Supplementary Material Access the most recent supplemental material at:
<http://cancerimmunolres.aacrjournals.org/content/suppl/2019/02/06/2326-6066.CIR-18-0419.DC1>

Cited articles This article cites 44 articles, 21 of which you can access for free at:
<http://cancerimmunolres.aacrjournals.org/content/7/4/600.full#ref-list-1>

E-mail alerts [Sign up to receive free email-alerts](#) related to this article or journal.

Reprints and Subscriptions To order reprints of this article or to subscribe to the journal, contact the AACR Publications Department at pubs@aacr.org.

Permissions To request permission to re-use all or part of this article, use this link
<http://cancerimmunolres.aacrjournals.org/content/7/4/600>.
Click on "Request Permissions" which will take you to the Copyright Clearance Center's (CCC) Rightslink site.